Organic & Supramolecular Chemistry

Cu^{II} Anchored onto the Magnetic Talc: A New Magnetic Nanostructured Catalyst for the One-Pot Gram-Scale Synthesis of 1*H*-Pyrazolo[1,2-b]phthalazine-5,10-dione Derivatives

Samaneh B. Chalaki and Batool Akhlaghinia*[a]

In the present study Cu^{II} anchored onto the magnetic talc (γ-Fe_2O_3/ talc /Cu^{II} NPs) was successfully synthesized and characterized by FT-IR, XRD, TEM, FE-SEM, EDX, VSM, and ICP-OES techniques. Structural characterizations reveal that the γ-Fe_2O_3/ talc/Cu^{II} NPs are superparamagnetic in nature, structured as a composite with average diameter of about 19–31 nm. The prepared nanostructured catalyst efficiently catalyzed the preparation of 1*H*-pyrazolo[1,2-b] phthalazine-5,10-diones at the gram scale without the use of the toxic organic solvents. The magnetically separable and environmentally friendly nanostructured catalyst remains quite stable during reaction conditions and reused for at least five recycle runs.

Introduction

Nitrogen-containing heterocyclic compounds occur widely in nature. In the past few decades, their applications in biologically active pharmaceuticals, agrochemicals, and functional materials are turning out to be prominent.[1–4] Among a large variety of *N*-heterocycles, those containing a pyrazole ring are of great interest because they exhibit a wide spectrum of pronounced pharmacological and biological activities.[5–8] Similarly, phthalazine derivatives due to their wide range of interesting properties such as anticonvulsant, cardiotonic, vasorelaxant, cytotoxic, antimicrobial, antifungal, anticancer and anti-inflammatory activities have attracted extensive attention.[9–16] As evidence, it has been reported that the titled compounds, 1*H*-pyrazolo[1,2-b]phthalazine-5,10-diones possess analgesic, antihypoxic and antipyretic activities.[17] In view of their wide utility range, the development of simple synthetic methods for the preparation of 1*H*-pyrazolo[1,2-b]phthalazine-5,10-diones is, therefore, an interesting challenge. Synthesis of 1*H*-pyrazolo[1,2-b]phthalazine-5,10-diones *via* multicomponent reaction (MCRs) is a powerful tool due to its advantages of the intrinsic atom economy, simple procedure, structural diversity, energy saving, and reduced waste.[18–20] To the best of our knowledge, there are only several works of literature about the multicomponent reactions of phthalhydrazide, malononitrile with aldehydes[19–22] in the presence of diverse catalysts such as PTSA/[Bmim]Br,[23] Et_3N/EtOH,[4] [Bmim]OH/MW,[24] 1,8-diazabicyclo[5,4,0]-undec-7-en-8-ium acetate, DBU[CH_3CO_2],[25] Al-KIT-6,[19] $NiCl_2.6H_2O$,[26] $InCl_3$,[27] CuI NPs,[28] TBBDA or PBBS,[29] CAN PEG 400,[30] $Ni_{0.5}$ $Zn_{0.5}$ Fe_2O_4 nano-crystallites,[31] SBA@BiPy^{2+} 2Cl^-,[32] RH@[SiPrDABCO@BuSO_3H]HSO_4,[33] ZrO_2 NPs,[34] PbO NPs,[35] ZnO NPs,[36] DCDBTSD,[37] DMAP,[38] β-Cyclodextrin,[39] $NaHCO_3$,[40] *p*-toluenesulfonic acid,[41] and Fe_3-*x*Ti*x*O_4@ SiO_2@urea MNPs.[42] Despite the merits of the previously reported synthetic methods, the generality of some of the known procedures is somewhat defected by using catalysts and solvents which are not acceptable in the context of green chemistry. Thus, further studies and development of novel methodologies are still necessary for overcoming the problems relating to environmental pollution which being encountered by the global population. Taking all these facts into account, designing and preparation of natural-based renewable heterogeneous nanocatalysts are an important strategy for the synthesis of 1*H*-pyrazolo[1,2-b]phthalazine-5,10-diones. One of the most crucial steps in designing a catalytic system is the choice of efficient support as the catalytic activity, selectivity and recycling of catalysts may be efficiently improved by support.

Clay minerals as abundant and cheap resources distributed worldwide, generate a great deal of interest in many different fields including adsorption,[43] catalysis,[44,45] nanocomposites,[46,47] tissue engineering, pharmaceuticals,[48,49] oil drilling and isolation industries.[50] Clay minerals with layered structure belong to the phyllosilicates group and based on the arrangement of tetrahedral silicate sheets and octahedral hydroxide sheets can be classified.[51,52] Talc with the well-known 2:1 type layered configuration has the chemical formula $Mg_3Si_4O_{10}(OH)_2$.[53] Talc composed of an octahedral magnesium hydroxide sheet sandwiched between two tetrahedral silica sheets in which the components bonded together by ionic and covalent bonds. Talc as a monoclinic and/or triclinic mineral[54] without residual surface charge[55] contains few –SiOH and –MgOH groups on the lateral faces, which represent Brønsted acidic sites.[56] On the other hand, the Si–O–Si bonds on the basal surface of talc display a low level of Lewis basicity. By

[a] *S. B. Chalaki, Dr. B. Akhlaghinia*
Department of Chemistry
Faculty of Science, Ferdowsi University of Mashhad, Mashhad 9177948974, Iran
E-mail: akhlaghinia@um.ac.ir

Supporting information for this article is available on the WWW under https://doi.org/10.1002/slct.202002099

considering the chemically active sites in the structure of talc, it can be used as excellent support for various heterogeneous catalysts.

As regards the time-consuming separation of talc by conventional approaches (centrifugation and filtration) from the reaction mixture and to prevent losing the heterogeneous catalyst during the separation process, the incorporation of magnetic nanoparticles (MNPs) into the talc structure[57] provides easy separation of catalysts from the reaction mixture using a simple magnetic bar. In addition, the application of magnetic nanoparticles (MNPs) in organic transformations has been developed due to their easy functionalization, large surface area ratio as well as low toxicity and price.[58,59]

In continuation of our studies on the synthesis and application of magnetic nanostructured catalysts[60–84] and to develop a new synthetic methodology for the preparation of 1*H*-pyrazolo[1,2-b]phthalazine-5,10-diones *via* one-pot multi-component reactions (MCRs), Cu^{II} anchored onto the magnetic talc (γ-Fe_2O_3/ talc/Cu^{II} NPs) as a magnetically heterogeneous nanocatalyst from commercially available chemicals in multiple steps was prepared. (Scheme 1) The method consists of the reaction between a mixed salt-solution of ferrous and ferric ions and NaOH in the presence of talc powder (**I**) as promising supporting material for catalysts in organic reactions. Afterward, the obtained Fe_3O_4/talc was heated at 220 °C for 3 h to produce γ-Fe_2O_3/talc NPs (**II**). Subsequently, Cu^{II} anchored onto the magnetic talc (γ-Fe_2O_3/talc/Cu^{II} NPs (**III**)) was obtained upon the treatment of γ-Fe_2O_3/talc NPs (**II**) with refluxing solution of $Cu(OAc)_2.H_2O$ in methanol.

Results and Discussion

In the first part of this paper, the preparation of γ-Fe_2O_3/talc/Cu^{II} NPs (**III**) was established by performing different analytical methods such as Fourier transform infrared (FT-IR) spectroscopy, X-ray diffraction (XRD), transmission electron microscopy (TEM), field emission scanning electron microscopy (FE-SEM), energy-dispersive X-ray (EDX), vibrating sample magnetometer (VSM), and inductively coupled plasma optical emission spectrometry (ICP-OES). In the second part, we illustrated the catalytic activity of γ-Fe_2O_3/talc/Cu^{II} NPs (**III**)) in the preparation of 1*H*-pyrazolo[1,2-b]phthalazine-5,10-diones *via* one-pot multi-component reaction under solvent-free conditions.

Preparation of Cu^{II} anchored onto the magnetic natural talc (γ-Fe_2O_3/talc/Cu^{II} NPs) can be confirmed by FT-IR spectroscopy. (Figure 1) The FT-IR spectra of the talc (**I**) (a), γ-Fe_2O_3/talc NPs (**II**) (b), γ-Fe_2O_3/talc/Cu^{II} NPs (**III**) (c), and 5th reused γ-Fe_2O_3/talc/Cu^{II} NPs (**III**) (d) are illustrated in Figure 1. As it is evident in Figure 1a, a sharp absorption band at 3676 cm^{-1} is related to the OH symmetric stretching vibrations of –SiOH and –MgOH groups on the lateral faces of talc.[85,86] Two adsorption bands appearing at 1018 cm^{-1} and 669 cm^{-1} correspond to the asymmetric and symmetric stretching vibrations of the Si–O–Si bond on the basal surface of talc. Furthermore, an absorption band at 466 cm^{-1} is assigned to the bending vibration of Si–O–Si bond.[85,86] The vibrational frequencies of Mg–O bond (in octahedral layer) appears at 675 and 458 cm^{-1}.[85,86] In the FT-IR spectrum of talc/γ-Fe_2O_3 NPs (**II**) (Figure 1b), the presence of γ-Fe_2O_3 in the talc structure can be identified by the band appearing around 620–570 cm^{-1} (corresponding to the stretching vibration of Fe–O bonds), which is covered by stretching vibrations of Si–O and Mg–O bonds.[75] Finally, the coordination of $Cu(OAc)_2.H_2O$ can be confirmed by the stretching vibrations that appear at 1558 and 1448 cm^{-1} (corresponding to asymmetric and symmetric stretching vibrations of acetate ions (OAc)) and 450 cm^{-1} (corresponding to stretching vibrations of Cu–O bond).[75] The latter absorption band is covered by the bending vibration frequency of Si–O–Si. Furthermore, this coordination can be verified by decreasing the intensity and frequency of the hydroxyl groups (Figure 1c).

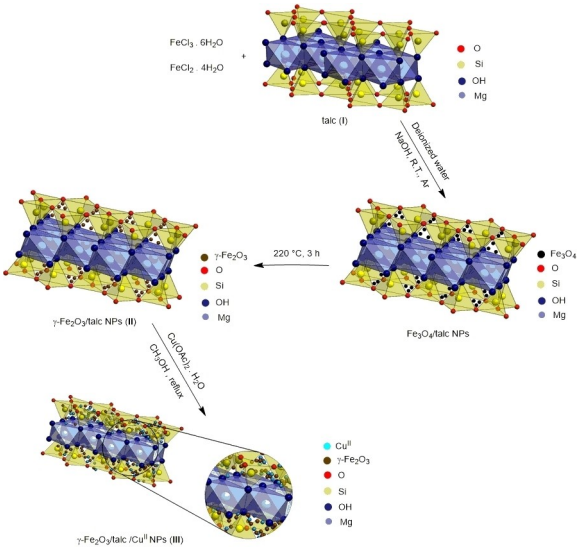

Scheme 1. Preparation of Cu^{II} anchored onto the magnetic natural talc (γ-Fe_2O_3/talc/Cu^{II} NPs (**III**)).

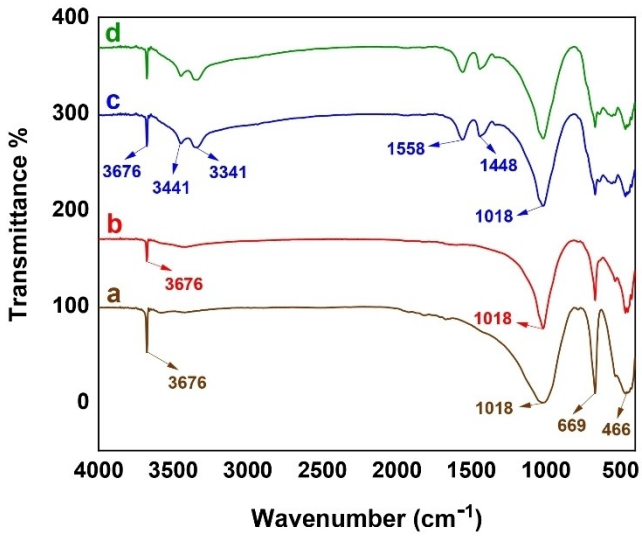

Figure 1. FT-IR spectra of the talc (**I**) (a), γ-Fe_2O_3/talc NPs (**II**) (b), γ-Fe_2O_3/talc/Cu^{II} NPs (**III**) (c), 5th reused γ-Fe_2O_3/talc/Cu^{II} NPs (d).

The crystalline structures of the γ-Fe_2O_3 (a), γ-Fe_2O_3/talc NPs (**II**) (b), and γ-Fe_2O_3/talc/Cu^{II} NPs (**III**) (c) were characterized by XRD technique (Figure 2). Figure 2a shows the typical diffraction peaks around $2\theta = 30.27°$ (2 0 6), 35.7° (1 1 9), 57.4° (1 1 15), and 63° (4 0 12) which can be confirmed the cubic spinel crystal structure of γ-Fe_2O_3 (Ref. Code: 00-025-1402). As can be evident from Figure 2b, the appearance of the characteristic peaks at $2\theta = 9.6°$ (0 0 1), 19.12° (0 0 2) and 28.55° (0 0 3) are imputed to the crystallization of the talc with an octahedral and tetrahedral unit cell (Ref. Code: 04-010-7170).[86] Similarly (in Figure 2a), the diffraction peaks appearing at $2\theta = 30.27°$ (2 0 6), 35.8° (1 1 9) and 63.01° (4 0 12) are associated to the γ-Fe_2O_3 (Ref. Code: 00-025-1402). It is worth mentioning, as it is evident from Figure 2c, due to the modification process, the intensities and positions of diffraction peaks were changed. In comparison, the crystallinity value and intensity of all peaks were decreased due to deformation of hydrogen bonding in the anchoring of Cu^{II} onto the magnetic talc, which was appeared as a diffraction peak at $2\theta = 43.58°$ (1 1 1) (Ref. Code: 00-004- 0836). According to the Debye-Scherrer equation $d = K\lambda/(\beta\cos\theta)$, the crystalline size of γ-Fe_2O_3/talc/Cu^{II} NPs (**III**) was estimated to be 25 nm.

Also, the TEM technique was carried out to obtain the direct information about the structure and morphology of γ-Fe_2O_3/talc/Cu^{II} NPs (**III**). Figures 3 and 4 represent the TEM images and particle size distributions of the synthesized γ-Fe_2O_3/talc/Cu^{II} NPs (**III**). As shown in Figure 3, the γ-Fe_2O_3 nanoparticles were distributed inside the talc cavities. Furthermore, a distribution histogram of γ-Fe_2O_3/talc/Cu^{II} NPs (**III**) revealed that the average diameter of the nanoparticles is 19–31 nm, which is in good agreement with the results deduced from XRD (Figure 4).

The magnetic property of γ-Fe_2O_3/talc/Cu^{II} NPs (**III**) was investigated using a vibrating sample magnetometer (VSM). As illustrated in Figure 5 the sample is superparamagnetic in nature.

It can be seen that the saturation magnetization value of γ-Fe_2O_3/talc/Cu^{II} NPs (**III**) is estimated to be 26 emu g^{-1}.

To further insights into the morphology of γ-Fe_2O_3/talc/Cu^{II} NPs (**III**), FE-SEM analysis was performed. As can be seen in Figure 5 (a and b), the as-synthesized γ-Fe_2O_3/talc/Cu^{II} NPs (**III**)

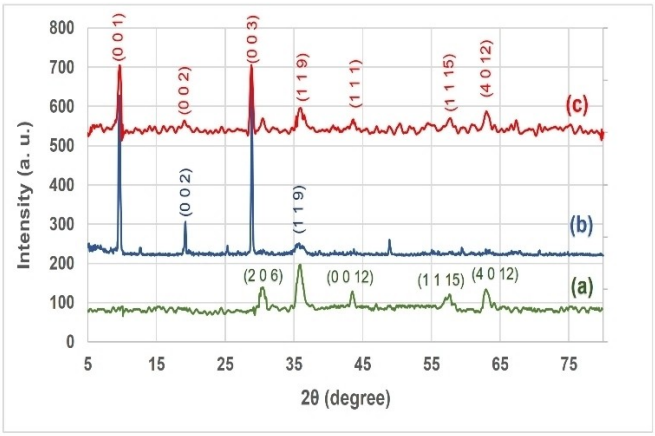

Figure 2. The XRD patterns of γ-Fe_2O_3 (a), γ-Fe_2O_3/talc NPs (**II**) (b), γ-Fe_2O_3/talc/Cu^{II} NPs (**III**) (c).

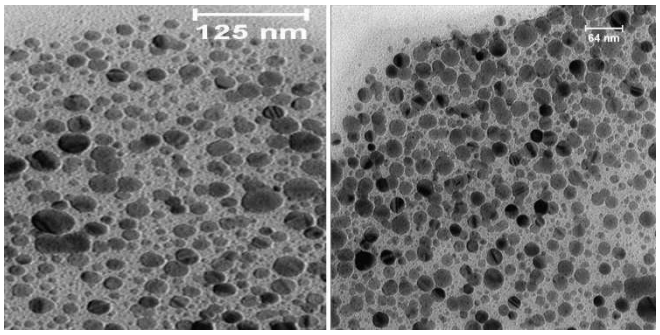

Figure 3. TEM images of γ-Fe_2O_3/talc/Cu^{II} NPs (**III**).

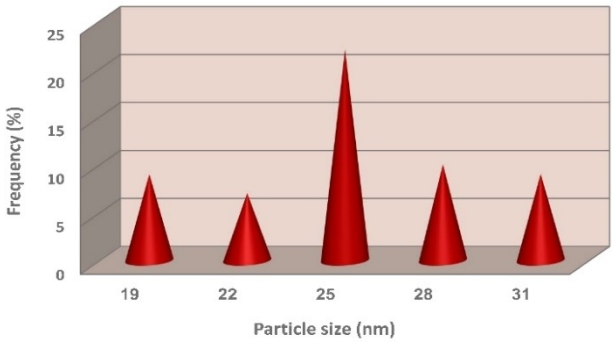

Figure 4. Particle size distribution histogram of γ-Fe_2O_3/talc/Cu^{II} NPs (**III**).

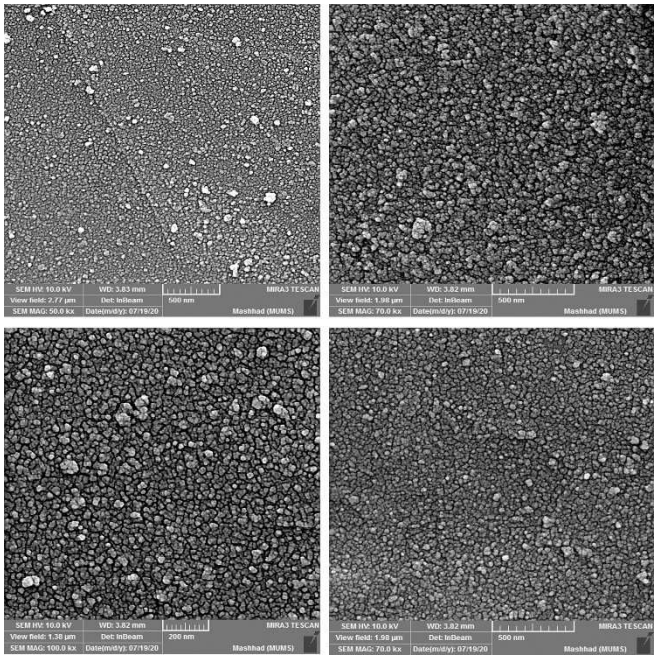

Figure 5. FE-SEM images of γ-Fe_2O_3/talc/Cu^{II} NPs (III) (a and b) and the 5th reused of γ-Fe_2O_3/talc/Cu^{II} NPs (III) (c and d).

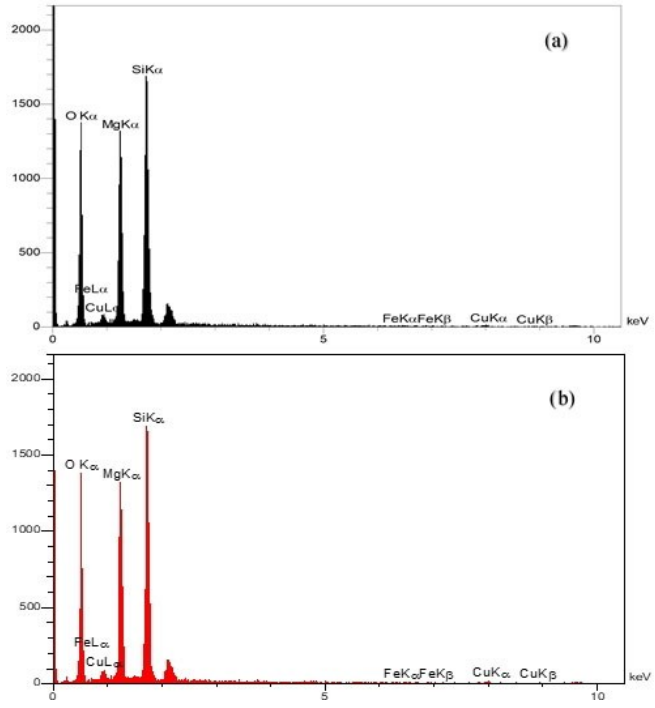

Figure 6. EDX spectrum of γ-Fe_2O_3/talc/Cu^{II} NPs (**III**) (a) and the 5th reused γ-Fe_2O_3/talc/Cu^{II} NPs (**III**) (b).

exhibited an irregular and amorphous morphology with good dispersion.

The type of elements in the γ-Fe_2O_3/talc/Cu^{II} NPs (**III**) structure was recognized using the energy-dispersive X-ray (EDX) technique. According to the data which is shown in Figure 6a, the presence of Si, Mg, Fe, Cu and O confirmed in the γ-Fe_2O_3/talc/Cu^{II} NPs (**III**) composition (Figure 6a).

The magnetic property of γ-Fe_2O_3/talc/Cu^{II} NPs (**III**) was investigated using a vibrating sample magnetometer (VSM).

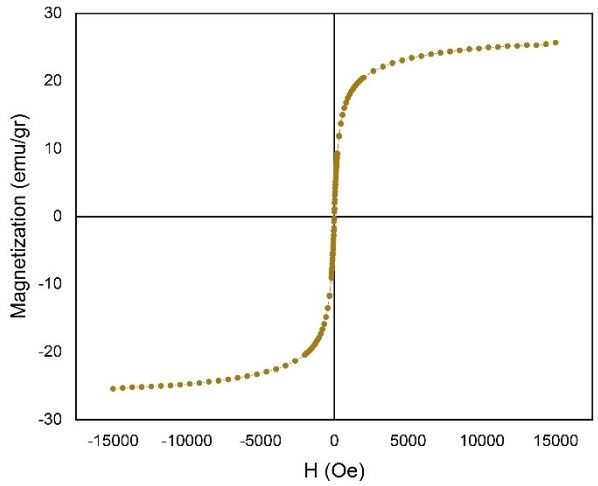

Figure 7. The magnetization curve of γ-Fe_2O_3/talc/Cu^{II} NPs (**III**).

As illustrated in Figure 7 the sample is superparamagnetic in nature.

It can be seen that the saturation magnetization value of γ-Fe_2O_3/talc/Cu^{II} NPs (**III**) is estimated to be 26 emu g^{-1}.

Catalytic synthesis of 1*H*-pyrazolo[1,2-b] phthalazine-5,10-diones in the presence of γ-Fe_2O_3/talc/Cu^{II} NPs (III)

Considering the modern 'paradigm shift' towards green synthesis, multicomponent reactions (MCRs) using magnetic nanostructured catalyst under solvent-free conditions have attracted more and more attention in synthetic organic chemistry. So, the catalytic activity of γ-Fe_2O_3/talc/Cu^{II} NPs (**III**) was investigated in the reaction of phthalhydrazide, malononitrile with aromatic and heteroaromatic aldehydes (Scheme 2).

Therefore, to establish the conditions for the synthesis 1*H*-pyrazolo[1,2-b] phthalazine-5,10-diones, the one-pot condensation reaction between phthalhydrazide, malononitrile and benzaldehyde was chosen as model reaction.

To set the optimistic conditions, the effects of different reaction parameters like catalyst loading, reaction temperature and solvents on the yield and reaction rate were screened.

Based on the experimental results summarized in Table 1, the necessary involvement of the catalyst in the condensation reaction (under solvent-free conditions at 100 °C) was verified by conducting the model reaction in the absence of the catalyst and in the presence of talc (**I**), γ-Fe_2O_3 NPs and γ-Fe_2O_3/talc NPs (**II**) as well. After a prolonged reaction time, in the absence of the catalyst, all of the starting materials remain intact and no expected product was obtained. (Table 1, entry 1) The model reaction in the presence of talc (**I**), γ-Fe_2O_3 NPs and γ-Fe_2O_3/talc NPs (**II**) is sluggish to give 25%, 40% and 50% of 3-amino-5,10-dioxo-1- phenyl-5,10-dihydro-1*H*-pyrazolo[1,2-b] phthalazine-2-carbonitrile, respectively, at 100 °C. (Table 1, entries 2–4) Interestingly in the presence of 2.4 mol% (0.03 g) of γ-Fe_2O_3/talc/Cu^{II} NPs (**III**), the model reaction progressed very easily and gave the desired product in 95% yield after 10 min (Table 1, entry 5). Next, to optimize the reaction temperature, at the same reaction conditions the model reaction was carried out at different temperatures. It was found that high catalytic activity was exhibited at 50 °C in comparison to the eight different temperatures screened on model reaction. (Table 1, entries 6–12) We also investigated the effect of lowering and raising the mol% of the catalyst. (Table 1, entries 13–15) It was found that 1.6 mol% (0.02 g) of γ-Fe_2O_3/talc/Cu^{II} NPs (**III**) was optimum to carry out the desired transformation. Lowering the catalyst amount to 1.2 mol% (0.015 g) decreased the product yield to 50%, whereas there was no improvement in the yield by increasing the catalyst loading. Further, the catalytic efficiency of γ-Fe_2O_3/talc/Cu^{II} NPs (**III**) for the preparation of 3-amino-5,10-dioxo-1-phenyl-5,10-dihydro-1*H*-pyrazolo[1,2-b] phthalazine-2-carbonitrile was studied in H_2O and EtOH. (Table 1, entries 16–17) It was observed that the reaction did not proceed efficiently in H_2O and the same result was obtained by performing the model reaction in EtOH. Based on the experimental results summarized in Table 1, the optimum

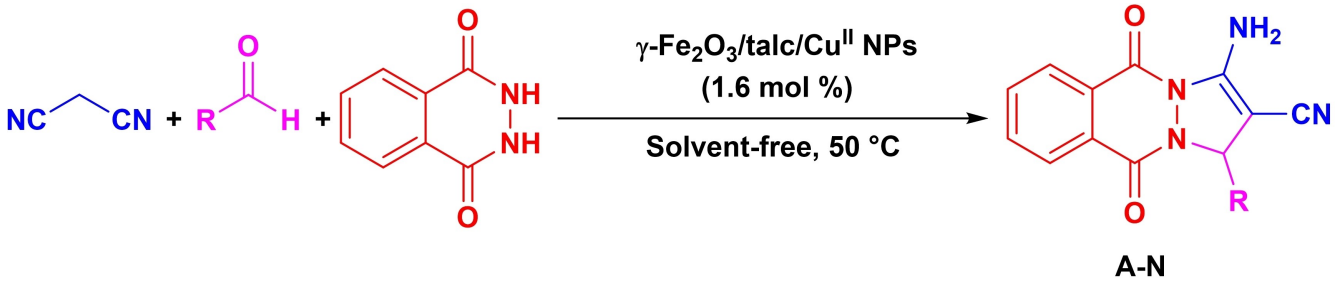

R: C_6H_5, 4-HOC_6H_5, 4-$O_2NC_6H_5$, 4-ClC_6H_5, 4-$H_3CC_6H_5$, 3,4-$(OH)_2C_6H_5$, 4-$CH_3OC_6H_5$, 4-pyridyl, 2-Thienyl, 2-furyl, 4-$(CH_3)_2NC_6H_5$

Scheme 2. γ-Fe_2O_3/talc/Cu^{II} NPs (**III**) catalysed synthesis of 1*H*-pyrazolo[1,2-b] phthalazine-5,10-diones.

Table 1. Synthesis of 3-amino-5,10-dioxo-1-phenyl-5,10-dihydro-1*H*-pyrazolo[1,2-b] phthalazine-2-carbonitrile in the presence of γ-Fe_2O_3/talc/Cu^{II} NPs (**III**) under different reaction conditions.

Entry	Catalyst (mol %)	Solvent	Temperature (°C)	Time (min)	Isolated yield %
1	—	–	100	24 h	–
2[a]	0.03 (g)	–	100	24 h	25
3[b]	0.03 (g)	–	100	8 h	40
4[c]	0.03 (g)	–	100	5 h	50
5	2.4	–	100	10	95
6	2.4	–	90	10	95
7	2.4	–	80	10	95
8	2.4	–	70	10	95
9	2.4	–	60	10	95
10	2.4	–	50	10	95
11	2.4	–	45	20	85
12	2.4	–	40	40	85
13	**1.6**	–	**50**	**10**	**95**
14	2.8	–	50	10	95
15	1.2	–	50	10	50
16	2.4	H_2O	50	8 h	10
17	2.4	EtOH	50	10	95
18[d]	1.6	–	50	50	90

[a] The reaction was performed in the presence of talc. [b] The reaction was performed in the presence of γ-Fe_2O_3. [c] The reaction was performed in the presence of γ-Fe_2O_3/talc NPs. [d] The reaction was performed in the presence of $Cu(OAc)_2.H_2O$.

conditions were thus to heat a 1:1:1 ratio of reactants in solvent-free conditions at 50 °C in the presence of 1.6 mol % of γ-Fe_2O_3/talc /Cu^{II} NPs (**III**). (Table 1, entry 13) Finally, to confirm the vital importance role of γ-Fe_2O_3/talc/Cu^{II} NPs (**III**) in the one-pot synthesis of 1*H*-pyrazolo[1,2-b] phthalazine-5,10-diones, the model reaction was performed in the presence of $Cu(OAc)_2.H_2O$ under the optimized reaction conditions. (Table 1, entry 18) Comparatively, the reaction in the presence of $Cu(OAc)_2.H_2O$ was slow and reasonable yield of the expected product was obtained after a longer reaction time.

In order to extend the scope and general applicability of this catalyst to a library system (Scheme 2), a series of variously substituted aldehydes were subjected to react with phthalhydrazide, and malononitrile under the aforementioned optimized conditions to furnish the corresponding1*H*-pyrazolo[1,2-b] phthalazine-5,10-diones. According to the results of Table 2, all the reactions were completed within 10–20 min to yield the respected products in relatively low reaction times and high yields. Generally, as seen in this table, the aromatic aldehydes bearing either electron-donating or electron-withdrawing groups underwent the reaction smoothly and afforded the products in high yields. It is obvious that the electron-withdrawing groups increase the reaction rate, which makes the aldehyde more electrophilic in the subsequent Michael addition in comparison with those carrying electron-donating groups. This can be attributed to the inductive and resonance electronic effects of the electron-withdrawing groups. Moreover, TOF and TON for the efficiency confirmation of the nanocatalyst were calculated and their results are summarized in Table 2.

All the prepared products according to the present protocol are known compounds. They are stable solids whose structures are fully characterized and identified by comparison of their melting points and mass spectra with the products prepared by the previously reported methods. To more clarification of the product structures, the structures of some selected 1*H*-

Table 2. One-pot synthesis of 1*H*-pyrazolo[1,2-b] phthalazine-5,10-diones under solvent-free conditions using γ-Fe_2O_3/talc/Cu^{II} NPs (**III**).

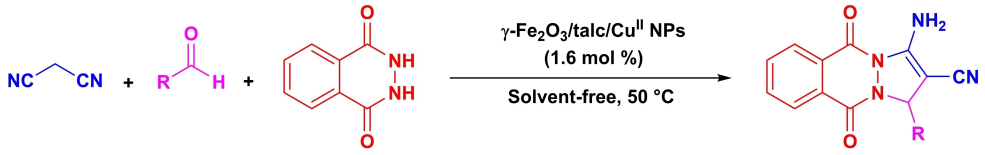

A-N

Entry	R	Product (A–N)	Time (min)	Isolated yield (%)	TON	TOF (h^{-1})
1	C_6H_5	A	10	95	41.30	6.88
2	4-HOC_6H_5	B	20	90	39.13	13.04
3	4-$O_2NC_6H_5$	C	10	96	41.74	6.96
4	3-BrC_6H_5	D	10	95	41.30	6.88
5	4-ClC_6H_5	E	10	94	40.87	6.81
6	4-$H_3CC_6H_5$	F	20	90	39.13	13.04
7	3, 4-$(OH)_2C_6H_5$	G	20	90	39.13	13.04
8	4-$CH_3OC_6H_5$	H	15	94	40.87	10.22
9	4-pyridyl	I	15	89	38.69	9.67
10	2-thienyl	J	20	91	39.56	13.19
11	2-furyl	K	18	92	40.00	12.00
12	4-$(H_3C)_2NC_6H_5$	L	20	90	39.13	13.04
13	HC=CHC_6H_5	M	25	85	36.96	15.40
14	4-FC_6H_5	N	15	95	41.30	10.33

pyrazolo[1,2-b] phthalazine-5,10-diones are determined by FT-IR, ^1H & ^{13}C NMR spectroscopic methods. The characteristic data of the synthesized compounds are presented in the Supplementary Material.

According to the mass spectrometric data, the molecular ion peak of all the prepared products exhibited their respective *m/z* and some useful fragmentation information for each compound has been found as well.

Based on the documents reported in the literature previously,[5,33] a schematic mechanism for the catalytic activity of γ-Fe_2O_3/talc/Cu^{II} NPs in the synthesis of titled compounds should be postulated as shown in Scheme 3. Mechanistically, it is likely that the reaction proceeds in a stepwise manner. The essential catalytic activity of γ-Fe_2O_3/talc/Cu^{II} in the one-pot condensation reaction between phthalhydrazide, malononitrile and aldehydes may be attributed to the acidic active sites (Cu^{II}), as well as few –SiOH and –MgOH groups (as Brønsted acidic sites) present on the lateral surface of talc and low level of Lewis basic sites of Si–O–Si siloxane bonds on the basal surface of talc (**I**).[36] Firstly, aldehyde and malononitrile undergo Knoevenagel condensation reaction in the presence of γ-Fe_2O_3/talc/Cu^{II} NPs to obtain the benzylidene malononitrile intermediate **I**. Subsequently, Michael addition of phthalhydrazide to the C=C bond of the electron-deficient Knoevenagel adduct **I** promoted by the nanostructured catalyst produced iminomethylene **II**. Finally, the intermediate **III** was obtained upon concerted intramolecular cyclization of iminomethylene **II** followed by the tautomeric transformation which leads to the corresponding1*H*-pyrazolo[1,2-b] phthalazine-5,10-diones as the more stable tautomer **IV**.

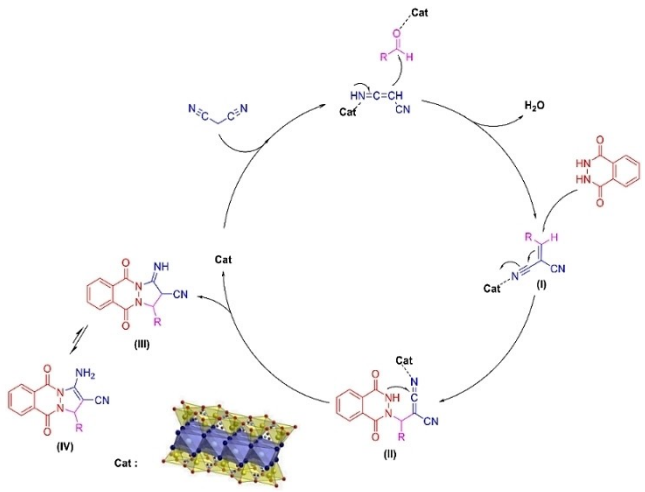

Scheme 3. Proposed reaction mechanism for the synthesis of 1*H*-pyrazolo [1,2-b] phthalazine-5,10-diones in the presence of γ-Fe_2O_3/talc/Cu^{II} NPs.

To confirm the importance of the industrial-scale application of the synthesized nanocatalyst, herein, a 50 gram-scale preparation of the pure 3-amino-5,10-dioxo-1-phenyl-5,10-dihydro-1*H*-pyrazolo[1,2-b] phthalazine-2-carbonitrile under the optimal conditions was reported. The typical procedure in detail was shown in the experimental section. The high catalytic activity of γ-Fe_2O_3/talc/Cu^{II} nanocatalyst than the previously reported nanocatalysts shows superior performance in the synthesis and purification of the desired product.

To investigate the maintenance of catalytic activity, the catalyst recovery and reusability were studied on model reaction under the optimized reaction conditions. In this procedure, when the reaction was completed, the reaction mixture was diluted with ethanol and the catalyst was separated from the reaction mixture by an external magnetic field. The recovered catalyst was washed with distilled water, then dried at 100 °C for 2 h, and tested for its activity in the subsequent run (Figure 8). The results were shown that γ-

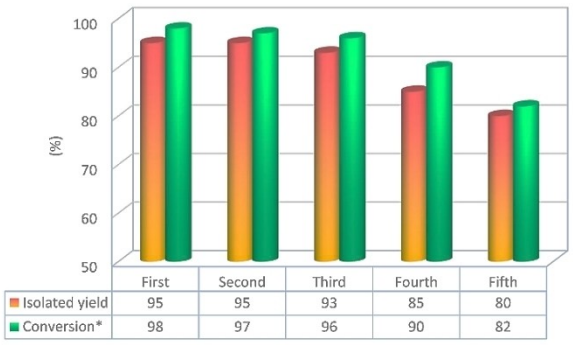

Figure 8. Synthesis of 3-amino-5,10-dioxo-1-phenyl-5,10-dihydro-1*H*-pyrazolo [1,2-b] phthalazine-2-carbonitrile in the presence of reused γ-Fe_2O_3/talc/Cu^{II} NPs (**III**).

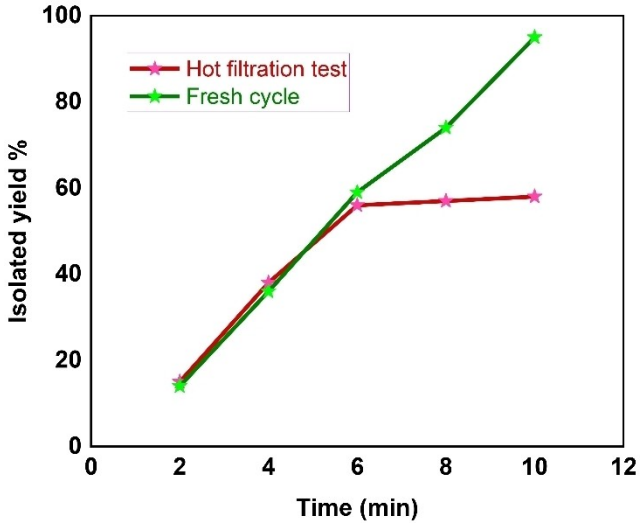

Figure 9. Time-dependent correlation of the product yield in hot filtration test.

Fe_2O_3/talc/Cu^{II} NPs (**III**) does not show any loss in its activity in the one-pot multicomponent reaction of malononitrile, phthalhydrazide, and benzaldehyde and the expected product was obtained in 95, 95, 93, 85, and 80% isolated yields, respectively. As shown in Figure 8, the catalyst could be used five times without a significant loss in its catalytic activity.

To confirm the stability of γ-Fe_2O_3/talc/Cu^{II} NPs (**III**) after 5 recycle from the reaction, any structural changes were investigated *via* FT-IR, FE-SEM, EDX and ICP-OES analysis. The FT-IR spectrum of the 5th reused catalyst was recorded and compared with that of the fresh catalyst (Figure 1d). The apparent resemblance between the FT-IR spectra of the fresh and the 5th reused catalyst authorized the maintenance of the catalyst activity. Moreover, no agglomeration was observed, according to the FE-SEM data which are shown in Figure 5 c and d. Likewise, the presence of Si, Mg, Fe, Cu and O elements in the composition of 5th reused γ-Fe_2O_3/talc/Cu^{II} NPs (**III**) clearly authenticated the composition stability of this nanostructured catalyst (Figure 6b).

Furthermore, the ICP-analysis of the 5th recycled catalyst reveals that the copper content of the 5th reused catalyst (4.9 wt.%) is less than that of fresh catalyst (5.1 wt.%).

Heterogeneity Studies

Hot Filtration Test

To demonstrate the possibility of leaching of the active species from the catalyst surface into the catalytic mixture, a hot filtration test has been conducted for the one-pot multicomponent reaction of malononitrile, phthalhydrazide, and benzaldehyde as a representative reaction (Figure 9). To this point, the model reaction was performed under the optimal conditions. Mid-way through each reaction (5 min), the catalyst was separated magnetically and the reaction was again continued for a further time (5 min). No further formation of 3-amino-5,10-dioxo-1-phenyl-5,10-dihydro-1*H*-pyrazolo[1,2-b] phthalazine-2-carbonitrile took place when the reaction progress was followed using thin-layer chromatography. Further, ICP-OES analysis revealed a negligible amount of Cu leached out during the entire course of the catalytic reaction (less than 0.05 wt.%). This result proved that γ-Fe_2O_3/talc/Cu^{II} NPs (**III**) is truly heterogeneous in nature, which highlights the sustainability of the system.

Poisoning test

To further explore the true nature of the as-synthesized nanostructured catalyst, a poisoning test was performed. For this purpose, the model reaction was carried out under the optimized reaction conditions in the presence and absence of ethylendiaminetetraacetic acid (EDTA) as an effective scavenger to hold the homogeneous copper species. The high affinity of EDTA to grab the soluble Cu^{II} ions leads to the formation of a stable complex (Scheme 4), which deactivates the leached-out copper species. According to the obtained results, if any significant decrease in the reaction efficiency was not observed, clearly proves that no Cu leaching occurred during the course of reaction and the reaction was likely to continue through a heterogeneous pathway. In this regard, the reaction progress

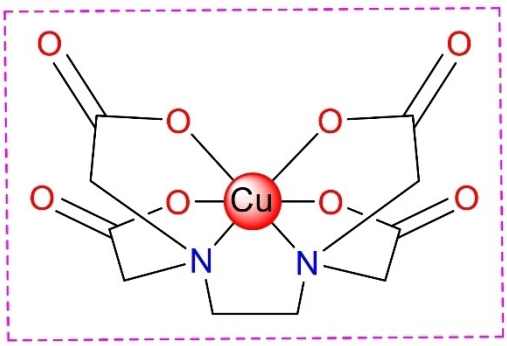

Scheme 4. The chemical structure of the copper (**II**) EDTA complex.

was monitored by TLC and the results are demonstrated in Figure 10. In accordance with these results, affording the corresponding product without any detectable decrease in the yield of the reaction clearly corroborated that no leaching of copper ions takes place during the reaction and the reaction arguably proceeds in a heterogeneous pathway. Considering these results, it is now beyond any doubt that the γ-Fe_2O_3/talc/Cu^{II} NPs (**III**) catalyst is purely heterogeneous in nature under the described reaction conditions.

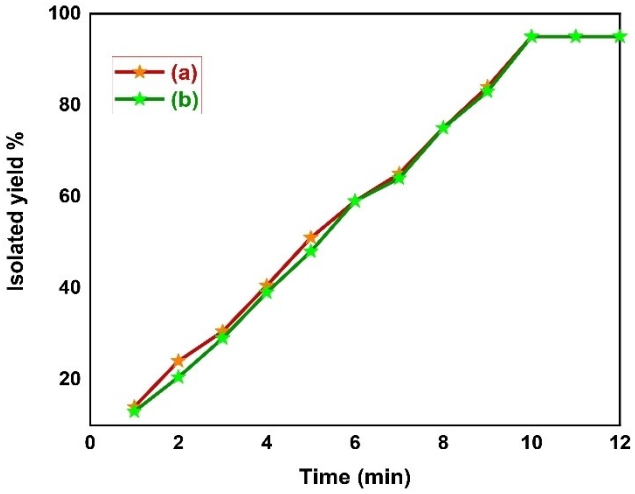

Figure 10. Product yield as a function of reaction time catalyzed by γ-Fe_2O_3/talc/Cu^{II} NPs (**III**) in (a) the absence and (b) the presence of EDTA.

The productivity and superiority of the present heterogeneous catalytic framework (γ-Fe_2O_3/talc/Cu^{II} NPs (**III**)) in the one-pot multicomponent reaction of malononitrile, phthalhydrazide and benzaldehyde (under the optimized reaction conditions) are compared with a number of the previously reported catalysts including homogenous and heterogeneous ones as summarized in Table 3. As seen in Table 3, the comparison was in terms of catalyst, solvent, temperature, reaction time, and percentage yields. Comparatively, among the other methods in Table 3, the present investigation affords a truly green and mild process using a magnetic separable nanostructured catalyst at lower temperature, with high yield of the product in shorter reaction time (Table 3, entry 24). Obviously, some other methods despite their own advantages, suffer from drawbacks such as using homogenous catalysts (Table 3, entries 1–14, 19), synthesized supports (Table 3, entries 20–23), high temperatures (Table 3, 6–13, 15–21 and 23), ultrasonic irradiation (Table 3, entry 4) and long reaction times (Table 3, entries 4–6, 8, 10, 12, 14, 18–20, 22, and 23).

Conclusion

In summary, we have skillfully synthesized γ-Fe_2O_3/talc/Cu^{II} NPs (**III**) as a stable, highly efficient, and reusable magnetic nanostructured catalyst for the preparation of 1*H*-pyrazolo[1,2-b] phthalazine-5,10-diones *via* one-pot multicomponent reaction (MCRs). Structural characterizations including FT-IR, XRD, TEM VSM, and ICP-OES techniques suggest that this nanostructured catalyst is superparamagnetic in nature, structured as a

Table 3. Comparison between efficiency of γ-Fe_2O_3/talc/Cu^{II} NPs (**III**) and some other catalysts for the synthesis of 3-amino-5,10-dioxo-1-phenyl-5,10-dihydro-1*H*-pyrazolo[1,2-b] phthalazine-2-carbonitrile.

Entry	Catalyst	Solvent	Temperature (°C)	Time (min)	Reusability	Yield (%)	Ref.
1	[Pyr][HCOO]	–	r.t.	14	–	93	19
2	DBU[CH_3COO]	–	r.t.	12	–	94	19
3	[Pyr][CH_3COO]	–	r.t.	14	–	94	19
4	Et_3N/Ultrasonic	EtOH	50	1 (h)	–	91	24
5	[bmim]OH	EtOH	60	1.5 (h)	–	93	25
6	*p*-toluenesulfonic acid	[bmim]Br	100	3 (h)	–	94	23
7	$NaHCO_3$	–	120	35	–	88	41
8	β-Cyclodextrin	H_2O:EtOH	80	2.5 (h)	3	93	40
9	$InCl_3$	–	80	25	–	94	28
10	$NiCl_2.6H_2O$	EtOH	Reflux	3 (h)	–	90	27
11[a]	TBBDA	–	80	15	–	89	30
12[b]	DMAP	EtOH	Reflux	1 (h)	–	96	39
13[c]	DCDBTSD	H_2O	80	30	–	80	38
14	CAN	PEG 400	r.t.	50	3	92	31
15	CuI NPs	–	92	25	–	92	29
16	ZnO NPs	–	100	14	–	90	37
17	PbO NPs	–	80	15	6	95	36
18	ZrO_2 NPs	–	100	45	–	91	35
19[d]	RH@[SiPrDABCO@$BuSO_3H$]HSO_4	EtOH	Reflux	3 (h)	–	89	34
20	SBA@$BiPy^{2+}$ $2Cl^-$	–	100	40	7	96	33
21	$Ni_{0.5}Zn_{0.5}Fe_2O_4$@HAP-Cs_2CO_3	–	110	15	5	93	32
22	Al-KIT-6	EtOH	60	4 (h)	4	93	26
23	$Fe_{3-x}TixO_4$@SiO_2@urea MNPs	EtOH:H_2O	Reflux	40	6	98	43
24	γ-Fe_2O_3/talc/Cu^{II} NPs	–	50	10	7	95	Present study

[a] *N,N,N′,N′*-tetrabromobenzene- 1,3-disulfonamide. [b] Dimethyldiazzomethylphosphonate. [c] *N*,2-dibromo-6-chloro-3,4-dihydro-2*H*-benzo[e][1,2,4] thiadiazine-7-sulfonamide 1,1- dioxide. [d] Nano Bronsted solid acid containing double-charged diazoniabi-cyclo[2.2.2]octane chloride supported on nano rice husk silica.

composite with average diameter of about 19–31 nm. Clearly, this unique structure exhibited excellent activity in the preparation of 1*H*-pyrazolo[1,2-b] phthalazine-5,10-diones towards the desired products in high yields. Notably, the novel catalyst remains quite stable during reaction conditions and can be efficiently separated using an external magnetic field and reused for at least five recycle runs. Owning to the advantages of this protocol compared to other reported methods, the present methodology suggests extensive application in combinatorial chemistry as well as in the multicomponent green synthesis that affords one-pot synthesis of 1*H*-pyrazolo[1,2-b]phthalazine-5,10-dione derivatives. Moreover, this method does not involve the use of a hazardous organic solvent, so it can be classified as green chemistry.

Supporting Information Summary

Experimental section, FT-IR, ^{1}HNMR, ^{13}CNMR and Mass spectrum analysis of products were described.

Acknowledgements

The authors gratefully acknowledge the partial support of this study by Ferdowsi University of Mashhad Research Council.

Conflict of Interest

The authors declare no conflict of interest.

Keywords: Cu^{II} anchored onto the magnetic talc (γ-Fe_2O_3/talc/Cu^{II} NPs) · 1*H*-pyrazolo[1,2-b]phthalazine-5,10-diones · nanostructured catalyst · solvent-free

[1] E. C. Franklin, *Chem. Rev.* **1935**, *16*, 305–361.
[2] F. W. Bergstrom, *Chem. Rev.* **1944**, *35*, 77–277.
[3] F. W. Lichtenthaler, *Acc. Chem. Res.* **2002**, *35*, 728–737.
[4] M. R. Nabid, S. J. T. Rezaei, R. Ghahremanzadeh, A. Bazgir, *Ultrason. Sonochem.* **2010**, *17*, 159–161.
[5] F. Al, K. N. Zelenin, E. E. Lesiovskaya, I. P. Bezhan, B. A. Chakchir, *Pharm. Chem. J.* **2002**, *36*, 598–603.
[6] R. P. Jain, J. C. Vederas, *Bioorg. Med. Chem. Lett.* **2004**, *14*, 3655–3658.
[7] R. W. Carling, K. W. Moore, L. J. Street, D. Wild, C. Isted, P. D. Leeson, S. Thomas, D. O'Connor, R. M. McKernan, K. Quirk, *J. Med. Chem.* **2004**, *47*, 1807–1822.
[8] C. M. Pask, K. D. Camm, C. A. Kilner, M. A. Halcrow, *Tetrahedron Lett.* **2006**, *47*, 2531–2534.
[9] S. Grasso, G. De Sarro, A. De Sarro, N. Micale, M. Zappalà, G. Puja, M. Baraldi, C. De Micheli, *J. Med. Chem.* **2000**, *43*, 2851–2859.
[10] Y. Nomoto, H. Obase, H. Takai, M. Teranishi, J. Nakamura, K. Kubo, *Chem. Pharm. Bull.* **1990**, *38*, 2179–2183.
[11] N. Watanabe, Y. Kabasawa, Y. Takase, M. Matsukura, K. Miyazaki, H. Ishihara, K. Kodama, H. Adachi, *J. Med. Chem.* **1998**, *41*, 3367–3372.
[12] a) V. A. Chebanov, E. A. Muravyova, S. M. Desenko, V. I. Musatov, I. V. Knyazeva, S. V. Shishkina, O. V. Shishkin, C. O. Kappe, *J. Comb. Chem.* **2006**, *8*, 427–434; b) A. Dondoni, A. Massi, S. Sabbatini, V. Bertolasi, *J. Org. Chem.* **2002**, *67*, 6979–6994.
[13] J. Liu, J. Li, L. Zhang, L. Song, M. Zhang, W. Cao, S. Zhu, H. Deng, M. Shao, *Tetrahedron Lett.* **2012**, *53*, 2469–2472.
[14] J. S. Kim, H.-K. Rhee, H. J. Park, S. K. Lee, C.-O. Lee, H.-Y. P. Choo, *Bioorg. Med. Chem.* **2008**, *16*, 4545–4550.
[15] S. El-Sakka, A. H. Soliman, A. Imam, *Afinidad* **2009**, *66*, 167–172.
[16] C.-K. Ryu, R.-E. Park, M.-Y. Ma, J.-H. Nho, *Bioorg. Med. Chem. Lett.* **2007**, *17*, 2577–2580.
[17] J. Li, Y.-F. Zhao, X.-Y. Yuan, J.-X. Xu, P. Gong, *Molecules* **2006**, *11*, 574–582.
[18] J. Sinkkonen, V. Ovcharenko, K. N. Zelenin, I. P. Bezhan, B. A. Chakchir, F. Al-Assar, K. Pihlaja, *Eur. J. Org. Chem.* **2002**, *2002*, 2046–2053.
[19] G. Karthikeyan, A. Pandurangan, *J. Mol. Catal. A* **2012**, *361*, 58–67.
[20] A. Kumar, M. K. Gupta, M. Kumar, *Green Chem.* **2012**, *14*, 290–295.
[21] G. Shanthi, P. T. Perumal, *J. Chem. Sci.* **2010**, *122*, 415–421.
[22] J. Wang, X. Bai, C. Xu, Y. Wang, W. Lin, Y. Zou, D. Shi, *Molecules* **2012**, *17*, 8674–8686.
[23] R. Ghahremanzadeh, G. I. Shakibaei, A. Bazgir, *Chem. Informationsdienst* **2008**, *2008*, 1129–1132.
[24] D. S. Raghuvanshi, K. N. Singh, *Tetrahedron Lett.* **2011**, *52*, 5702–5705.
[25] H. R. Shaterian, M. Mohammadnia, *J. Mol. Liq.* **2012**, *173*, 55–61.
[26] S.-H. Song, J. Zhong, Y.-H. He, Z. Guan, *Tetrahedron Lett.* **2012**, *53*, 7075–7077.
[27] M. V. Reddy, Y. T. Jeong, *Tetrahedron Lett.* **2013**, *54*, 3546–3549.
[28] J. Safaei-Ghomi, H. Shahbazi-Alavi, A. Ziarati, R. Teymuri, M. R. Saberi, *Chin. Chem. Lett.* **2014**, *25*, 401–405.
[29] R. Ghorbani-Vaghei, S. Noori, Z. Toghraei-Semiromi, Z. Salimi, *RSC Adv.* **2014**, *4*, 47925–47928.
[30] M. Kidwai, R. Chauhan, *J. Heterocycl. Chem.* **2014**, *51*, 1689–1696.
[31] B. Maleki, S. Barat Nam Chalaki, S. Sedigh Ashrafi, E. Rezaee Seresht, F. Moeinpour, A. Khojastehnezhad, R. Tayebee, *Appl. Organomet. Chem.* **2015**, *29*, 290–295.
[32] A. Bashti, A. R. Kiasat, B. Mokhtari, *RSC Adv.* **2015**, *5*, 25816–25823.
[33] J. Davarpanah, A. R. Kiasat, *RSC Adv.* **2015**, *5*, 7986–7993.
[34] M. Piltan, *Heterocycl. Commun.* **2017**, *23*, 401–403.
[35] R. Tayebee, B. Maleki, *J. Iran. Chem. Soc.* **2017**, *14*, 1179–1188.
[36] A. Azarifar, R. Nejat-Yami, D. Azarifar, *J. Iran. Chem. Soc.* **2013**, *10*, 297–306.
[37] A. Khazaei, M. A. Zolfigol, F. Karimitabar, I. Nikokar, A. R. Moosavi-Zare, *RSC Adv.* **2015**, *5*, 71402–71412.
[38] E. Lamera, S. Bouacida, H. Merazig, A. Chibani, M. Le Borgne, Z. Bouaziz, A. Bouraiou, *Z. Naturforsch. B* **2017**, *72*, 361–368.
[39] Y. A. Tayade, D. S. Dalal, *Catal. Lett.* **2017**, *147*, 1411–1421.
[40] A. Vafaee, A. Davoodnia, M. Pordel, M. R. Bozorgmehr, *Oriental J. Chem.* **2015**, *31*, 2153–2158.
[41] R. Ghahremanzadeh, G. I. Shakibaei, A. Bazgir, *Letter* **2008**, *2008*, 1129–1132.
[42] D. Azarifar, O. Badalkhani, Y. Abbasi, M. Hasanabadi, *J. Iran. Chem. Soc.* **2017**, *14*, 403–418.
[43] H. Zaitan, A. Korrir, T. Chafik, D. Bianchi, *J. Hazard. Mater.* **2013**, *262*, 365–376.
[44] E. González, D. Rodríguez, L. Huerta, A. Moronta, *Clays Clay Miner.* **2009**, *57*, 383–391.
[45] N. Kaur, D. Kishore, *J. Chem. Pharm. Res.* **2012**, *4*, 991–1015.
[46] Y. Zhang, J. R. Evans, *Appl. Surf. Sci.* **2012**, *258*, 2098–2102.
[47] Y. Lvov, E. Abdullayev, *Prog. Polym. Sci.* **2013**, *38*, 1690–1719.
[48] W. Chrzanowski, S. Y. Kim, E. A. A. Neel, *Aust. J. Chem.* **2013**, *66*, 1315–1322.
[49] L. A. de Sousa Rodrigues, A. Figueiras, F. Veiga, R. M. de Freitas, L. C. C. Nunes, E. C. da Silva Filho, C. M. da Silva Leite, *Colloids Surf. B* **2013**, *103*, 642–651.
[50] J. T. Kloprogge, S. Komarneni, J. E. Amonette, *Clays Clay Miner.* **1999**, *47*, 529–554.
[51] R. T. Martin, S. W. Bailey, D. D. Eberl, D. S. Fanning, S. Guggenheim, H. Kodama, D. R. Pevear, J. Środoń, F. J. Wicks, *Clays Clay Miner.* **1991**, *39*, 333–335.
[52] D. Zhang, C.-H. Zhou, C.-X. Lin, D.-S. Tong, W.-H. Yu, *Appl. Clay Sci.* **2010**, *50*, 1–11.
[53] S. W. Bailey, *Clays Clay Miner.* **1969**, *17*, 355–371.
[54] K. Chabrol, M. Gressier, N. Pebere, M.-J. Menu, F. Martin, J.-P. Bonino, C. Marichal, J. Brendle, *J. Mater. Chem.* **2010**, *20*, 9695–9706.
[55] M. Bruno, M. Prencipe, G. Valdre', *Phys. Chem. Miner.* **2006**, *33*, 63–71.
[56] E. M. de C. Lobato, *Determination of Surface Free Energies and Aspect Ratio of Talc*, Virginia Tech, **2004**.
[57] K. Kalantari, M. B. Ahmad, K. Shameli, R. Khandanlou, *Int. J. Nanomed.* **2013**, *8*, 1817.

[58] S. Shylesh, V. Schuenemann, W. R. Thiel, *Angew. Chem. Int. Ed.* **2010**, *49*, 3428–3459; *Angew. Chem.* **2010**, *122*, 3504–3537.
[59] R. N. Baig, R. S. Varma, *Chem. Commun.* **2013**, *49*, 752–770.
[60] A. Mohammadinezhad, B. Akhlaghinia, *Green Chem.* **2017**, *19*, 5625–5641.
[61] R. Jahanshahi, B. Akhlaghinia, *RSC Adv.* **2016**, *6*, 29210–29219.
[62] M. Zarghani, B. Akhlaghinia, *RSC Adv.* **2016**, *6*, 38592–38601.
[63] Z. Zarei, B. Akhlaghinia, *RSC Adv.* **2016**, *6*, 106473–106484.
[64] R. Jahanshahi, B. Akhlaghinia, *Catal. Lett.* **2017**, *147*, 2640–2655.
[65] M. S. Ghasemzadeh, B. Akhlaghinia, *Bull. Chem. Soc. Jpn.* **2017**, *90*, 1119–1128.
[66] M. Nejatianfar, B. Akhlaghinia, R. Jahanshahi, *Appl. Organomet. Chem.* **2018**, *32*, e4095.
[67] Z. Zarei, B. Akhlaghinia, *New J. Chem.* **2017**, *41*, 15485–15500.
[68] Z. Zarei, B. Akhlaghinia, *Turk. J. Chem.* **2018**, *42*, 170–191.
[69] M. S. Ghasemzadeh, B. Akhlaghinia, *ChemistrySelect* **2018**, *3*, 3161–3170.
[70] M. Zamani, B. Akhlaghinia, A. Mohammadinezhad, *ChemistrySelect* **2018**, *3*, 9431–9442.
[71] M. S. Ghasemzadeh, B. Akhlaghinia, *ChemistrySelect* **2019**, *4*, 1542–1555.
[72] S. Pakdel, B. Akhlaghinia, A. Mohammadinezhad, *ChemistryAfrica* **2019**, *2*, 367–376.
[73] N. Razavi, B. Akhlaghinia, *RSC Adv.* **2015**, *5*, 12372–12381.
[74] S. S. Ghodsinia, B. Akhlaghinia, *RSC Adv.* **2015**, *5*, 49849–49860.
[75] M. Zarghani, B. Akhlaghinia, *Appl. Organomet. Chem.* **2015**, *29*, 683–689.
[76] R. Jahanshahi, B. Akhlaghinia, *RSC Adv.* **2015**, *5*, 104087–104094.
[77] N. Y. Siavashi, B. Akhlaghinia, M. Zarghani, *Res. Chem. Intermed.* **2016**, *42*, 5789–5806.
[78] M. Zarghani, B. Akhlaghinia, *RSC Adv.* **2016**, *6*, 31850–31860.
[79] M. Zarghani, B. Akhlaghinia, *Bull. Chem. Soc. Jpn.* **2016**, *89*, 1192–1200.
[80] A. Mohammadinezhad, B. Akhlaghinia, *Aust. J. Chem.* **2018**, *71*, 32–46.
[81] N. Mohammadian, B. Akhlaghinia, *Res. Chem. Intermed.* **2018**, *44*, 1085–1103.
[82] H. Karimzadegan, B. Akhlaghinia, M. S. Ghasemzadeh, *Iran. J. Catal.* **2019**, *9*, 109–120.
[83] B. Akhlaghinia, P. Sanati, A. Mohammadinezhad, Z. Zarei, *Res. Chem. Intermed.* **2019**, *45*, 3215–3235.
[84] M. S. Ghasemzadeh, B. Akhlaghinia, *New J. Chem.* **2019**, *43*, 5341–5356.
[85] A. M. A. Morsy, *Environ. Technol. Inno.* **2017**, *8*, 399–410.
[86] P. Marzbani, H. Resalati, A. Ghasemian, A. Shakeri, *BioResources* **2016**, *11*, 8720–8738.

Submitted: May 23, 2020
Accepted: September 9, 2020